Submitted to Physical Review

UCRL-19566
Preprint

c. 2

MULTIPLET SPLITTING OF METAL-ATOM ELECTRON BINDING ENERGIES

RECEIVED
LAWRENCE
RADIATION LABORATORY
APR 24 1970
LIBRARY AND
DOCUMENTS SECTION

C. S. Fadley and D. A. Shirley

April 1970

AEC Contract No. W-7405-eng-48

TWO-WEEK LOAN COPY

This is a Library Circulating Copy which may be borrowed for two weeks. For a personal retention copy, call Tech. Info. Division, Ext. 5545

UCRL-19566 c. 2

LAWRENCE RADIATION LABORATORY
UNIVERSITY of CALIFORNIA BERKELEY

37

DISCLAIMER

This document was prepared as an account of work sponsored by the United States Government. While this document is believed to contain correct information, neither the United States Government nor any agency thereof, nor the Regents of the University of California, nor any of their employees, makes any warranty, express or implied, or assumes any legal responsibility for the accuracy, completeness, or usefulness of any information, apparatus, product, or process disclosed, or represents that its use would not infringe privately owned rights. Reference herein to any specific commercial product, process, or service by its trade name, trademark, manufacturer, or otherwise, does not necessarily constitute or imply its endorsement, recommendation, or favoring by the United States Government or any agency thereof, or the Regents of the University of California. The views and opinions of authors expressed herein do not necessarily state or reflect those of the United States Government or any agency thereof or the Regents of the University of California.

MULTIPLET SPLITTING OF METAL-ATOM ELECTRON BINDING ENERGIES

C. S. Fadley and D. A. Shirley

Lawrence Radiation Laboratory
University of California
Berkeley, California 94720

April 1970

ABSTRACT

X-ray photoelectron spectroscopy (XPS) is used to measure splittings of metal-atom electron binding energies, in both inorganic solids and gases. These splittings are due to the various possible multiplet states formed by coupling a hole in a metal-atom subshell to an unfilled valence subshell.

Splittings are observed in various solids containing 3d series atoms. In particular, the 3s binding energy is split into a doublet with as much as 7.0 eV separation between the two components. The instrumental resolution is $\sim$ 1.0 eV. 3s splittings are exhibited by inorganic compounds containing Mn and Fe, as well as by Fe metal, Co metal, and Ni metal. Theoretical predictions are in good agreement with experiment, provided that the effects of covalency in chemical bonding are taken into account. For Fe metal, the 3s splitting is identical both above and below the Curie point. The 3p binding energies of these solids also appear to show multiplet effects, but the interpretation of these results is less straightforward. The 2p binding energies in MnF_2 are broadened by at least 1.3 eV, and this is shown to be consistent with multiplet splitting.

XPS results for gaseous monatomic Eu also indicate the presence of multiplet splittings. The two components in the 4d photoelectron

spectrum are found to have an intensity ratio in disagreement with observed ratios for neighboring atoms with filled valence subshells. Also, the width of the 4f photoelectron peak above the instrumental contribution can be explained in terms of multiplet effects.

A. Introduction

In any atomic system with unpaired valence electrons, the exchange interaction affects spin-up and spin-down core electrons unequally. Since exchange acts only between electrons with the same spin,[1] core electrons with spins parallel to those of the unpaired valence electrons will experience a valence-electron exchange potential, whereas core electrons with spins antiparallel will not. Since the exchange interaction tends to reduce the average Coulombic repulsion between two electrons,[1] the spin-parallel core electrons will be favored energetically. Exchange interactions within or between closed shells balance exactly, as the numbers of electrons with each spin are equal. This interaction between core and unpaired valence electrons is responsible for core-polarization contributions to magnetic hyperfine structure.[2] Due to the non-equivalent exchange interactions felt by core electrons with different spins, the spin-up and spin-down wave functions are slightly displaced spatially from one another.[2] In atomic iron, for example, the $3s\alpha$ and $3s\beta$ wavefunctions are predicted to have average radii of 0.433 Å and 0.435 Å respectively.[3] Here we have used α to denote a spin parallel to the unpaired 3d electrons. This relatively slight difference of $\sim 0.5\%$ in average radius creates a large net spin density at the nucleus. This spin density results in a large magnetic field in the Hamiltonian describing the hyperfine interactions between nucleus and electrons.[4] Numerous studies of the systematics of this hyperfine field have been made.[4,5]

In addition to slight spatial polarizations caused by unpaired valence electrons, the binding energies of core electrons should be

affected. Spin-unrestricted Hartree-Fock calculations predict differences in the spin-up and spin-down core-electron energy eigenvalues of transition metal ions.[2,3] Such differences are $\sim$ 12 eV for the 3sα and 3sβ electrons in atomic iron,[3] for example. It has been pointed out that these differences ought to be reflected as splittings in the measured binding energies of these electrons.[6] By means of x-ray photoelectron spectroscopy (XPS), which has a resolution of $\sim$ 1 eV, an attempt was made to detect such splittings in core-level photoelectron peaks from iron and cobalt metal.[6] However, no pronounced effects were observed.[6] Recently, splittings of $\sim$ 1 eV have been found in paramagnetic molecules[7] and larger effects have been observed in solids containing Mn and Fe.[8] In particular, Fadley, Shirley, Freeman, Bagus, and Mallow[8] observed $\sim$ 6 eV splittings in the 3s binding energies for the transition metal ions Mn^{2+} $3d^5$ and Fe^{3+} $3d^5$ in certain solids. These splittings are considerably reduced from free-ion predictions, and a major source of this reduction appears to be covalent-bonding effects.[8] The 3p binding energies in these solids also give evidence for splittings, but from both a theoretical and experimental point of view, the interpretation of this data is less straightforward.[8]

In this paper, we review the results obtained previously for Mn and Fe,[8] and also present data for 3s electrons in Co metal and Ni metal which indicate similar effects. Photoelectron spectra for the Mn2p electrons in MnF_2 are shown to exhibit similar, but smaller, splittings than Mn3s, as expected from free-ion theoretical calculations. We also discuss photoelectron spectra obtained from gaseous Eu which show certain anomalies

probably connected to such splittings. The experimental procedure is discussed in Section B. Experimental and theoretical results are presented and discussed in Section C. Our conclusions appear in Section D.

B. Experimental Procedure

The experimental procedure has been described elsewhere.[8,9] Samples were bombarded with x-rays of $\sim$ 1 keV energy (primarily with the unresolved $MgK\alpha_{1,2}$ doublet, which has an energy of 1.2536 keV). The ejected electrons were analyzed for kinetic energy in a magnetic spectrometer. The kinetic energy distributions obtained in this way contain photoelectron peaks corresponding to excitation from all the core and valence electronic levels in the sample whose binding energies are less than the excitation energy $h\nu$. The pertinent energy conservation equation is

$$h\nu = E^h - E^i + \varepsilon + \text{work function and charging corrections}, \quad (1)$$

where E^h is the total energy of the final state of the system with a hole in some subshell, E^i is the total energy of the initial state of the system, and ε is the kinetic energy of the electron ejected from that subshell. Work function and charging correction will accelerate or decelerate all electrons equally, and so can be disregarded in the measurement of splittings within a single sample.[9,10] The quantity $E^h - E^i$ is by definition the binding energy of an electron in the subshell, relative to the final hole state corresponding to E^h. If the ejection of an electron from a subshell can result in several final states of the system (i.e., several E^h values), a corresponding number of photoelectron peaks will be observed. Thus, the energy splittings of these final states are in principle directly measurable. The instrumental contribution to linewidth for these experiments was $\sim$ 1.0 eV full width at half-maximum intensity(FWHM). This width arises primarily from the natural width of the exciting radiation.

Measurements were made on several inorganic solids containing Mn and Fe, as these atoms possess a large number of unpaired d electrons (neutral atom electron configurations: Mn^0 - $3d^5 4s^2$, Fe^0 - $3d^6 4s^2$). Compounds were studied at room temperatures and a pressure of $\sim 10^{-5}$ torr. These samples were usually prepared by dusting the powdered crystal onto an adhesive backing to form a contiguous coating.[9] In a few cases, samples were prepared by painting an ethyl alcohol slurry of the powder directly on a metal backing.[9] Pure 3d series metals were also studied, and these samples were heated in a hydrogen atmosphere ($\sim 10^{-3}$ torr) to free them of surface oxidation.[6,9,11]

The choice of solid samples to be studied was restricted by two factors: (1) The sample must be in a vacuum if photoelectrons are to be analyzed for kinetic energy without appreciable inelastic scattering. (2) The vacuum in our spectrometer was rather poor, with pressures in the 10^{-5} torr range. These factors precluded the study of well-defined hydrated salts, as these salts will either lose water of hydration at room temperature or condense material from the residual gas in the system if cooled to very low temperatures. Also, transition metals which react to any degree with oxygen had to be reduced in an atmosphere of hydrogen.[6,9,11] For room temperature studies, anhydrous salts of metals with strongly electronegative anions represented the most useful samples. In certain cases, metal oxides were stable enough to be studied under the conditions of our experiments. Both iron and manganese have at least three oxides. From the point of view of observing multiplet splittings, the most desirable oxide of manganese is MnO, which contains Mn^{2+} ions in a

$3d^5\ ^6S$ electronic state. However, MnO is slightly unstable to oxidation by residual O_2 gas via the reactions:

$$3\ MnO + 1/2\ O_2 \rightarrow Mn_3O_4$$

and

$$2\ MnO + 1/2\ O_2 \rightarrow Mn_2O_3 \quad .$$

The other oxides of Mn and Fe are often non-stoichiometric and therefore do not constitute particularly well-defined systems. The metal halides present another possibility, but among these, only the fluorides have sufficient stability to be used with confidence. For example, the equilibrium constant for the reaction

$$MnCl_2 + O_2 \rightarrow MnO_2 + Cl_2$$

is $\sim 10^5$, while that for the reaction

$$MnF_2 + O_2 \rightarrow MnO_2 + F_2$$

is $\sim 10^{-50}$. MnF_2 and, to a lesser extent, FeF_3, thus represent good systems for the study of multiplet splittings. We have also studied the compounds MnO, MnO_2, $K_4Fe(CN)_6$, and $Na_4Fe(CN)_6$, for which no major chemical instability problems were noted. Minor effects of surface reaction are discussed below.

The monatomic gases[12] Eu and Yb were also studied.[9] Eu possesses a half-filled 4f shell (electron configuration Eu^0 - $4f^7 6s^2$) and might be expected to show splittings, whereas Yb has a filled 4f shell (Yb^0 - $4f^{14} 6s^2$),

and should not show these effects. A special oven was constructed for these experiments.[9] In this oven, solid metal was heated to a temperature at which the metal vapor pressure was $\sim 10^{-2}$ torr ($\sim$ 600°C for Eu and $\sim$ 540°C for Yb). At these conditions, reasonable photoelectron counting rates were obtained from the gas phase.[9] No significant Doppler broadening of photoelectron peaks should result at these temperatures.

The only form of data analysis applied to photoelectron spectra was a least-squares fit of empirically-selected, analytical peak shapes.[9] This procedure permitted accurate determinations of peak positions, widths, relative shapes, and intensities, and also of the importance of inelastic scattering effects. The selection of peak shapes has been described elsewhere.[9] The most useful shapes are Lorentzian or Gaussian with smoothly-connected constant tails of adjustable height on the low kinetic energy side. These tails represent reasonably well the effects of inelastic scattering on electrons escaping from the sample.[9] It was also possible in this fitting procedure to allow automatically for the effects of the weak $K\alpha_3$ and $K\alpha_4$ satellite x-rays separated by $\sim$ 10 eV from the main $K\alpha_{1,2}$ component in the Mg x-ray spectrum.[9] Photoelectron peaks due to these satellites are indicated as "$\alpha_{3,4}$" in Fig. 1, for example.

C. Results and Discussion

1. Solids Containing 3d Series Atoms

Figure 1 shows photoelectron spectra obtained from MnF_2, MnO, and MnO_2 in the region corresponding to ejection from the Mn3s and Mn3p core levels. Figure 2 shows spectra in a similar region from the iron-containing solids, FeF_3, Fe metal, $K_4Fe(CN)_6$ and $Na_4Fe(CN)_6$. The strong peaks in these spectra are labelled with the arbitrary notation 3s(1) 3s(2), ··· and 3p(1), 3p(2)···, unless they can be assigned to some obvious cause other than ejection from 3s or 3p levels by $MgK\alpha_{1,2}$ x-rays. In the latter category are the peaks due to the α_3 and α_4 satellite x-rays and the Na2s peak in $Na_4Fe(CN)_6$. The relative shifts in kinetic energy of the 3p(1) peaks in either Fig. 1 or Fig. 2 do not have special significance, as absolute energy measurements were not made with high precision. Therefore, some of these shifts could be due to such effects as charging of the sample. Within a given spectrum, however, relative peak locations can be determined quite accurately.

We concentrate first on the 3s regions of Figs. 1 and 2. Table I summarizes our experimental results as obtained by least-squares fits of Lorentzian-based peak shapes[9] to the data, and also gives the approximate free-ion electron configurations for the transition metal ions in these solids. Also noted in Fig. 2 and Table I are those cases for which known properties and/or the observation of broadening of certain photoelectron peaks seem to indicate slight chemical alteration of the sample. As the photoelectrons in the full-energy, inelastic peaks such as those labelled in Figs. 1 and 2 come from only a thin ($\sim 10^{-6}$ cm) surface layer of a solid

sample, a relatively small amount of surface reaction can alter photoelectron spectra appreciably.[6,9,10] For example, MnO_2 samples prepared from an ethyl-alcohol slurry exhibit an enhanced 3s(2) peak relative to samples prepared by dusting powder directly on an adhesive backing. The separation of the 3s(1) and 3s(2) peaks is the same for both cases, however. This change in relative intensity may be due to slight surface reduction in the alcohol, as noted in Table I. Spectra for MnF_2, on the other hand, exhibited no significant changes dependent upon sample preparation technique, and this is consistent with the higher chemical stability of this compound.

In the 3s region, the $3d^5$ compounds exhibit two peaks, denoted 3s(1) and 3s(2). MnO_2 shows a somewhat weaker 3s(2) peak at smaller separation. $K_4Fe(CN)_6$ and $Na_4Fe(CN)_6$ shows essentially no 3s(2) peak. Iron metal exhibits a distinct shoulder which persists with no appreciable change from 810°C (40°C above the Curie point) to 565°C, as shown in Fig. 3. (This shoulder was not observed in earlier work[6] due to poor statistics.) These results are fully consistent with the peaks 3s(1) and 3s(2) representing two final states of the Mn or Fe ion split primarily by the exchange interaction. That is, the 3s(2) peak is observed for cases where d electrons are known to couple to a high spin ground state (MnF_2, MnO, FeF_3, and ferromagnetic Fe) and is reduced in separation and intensity relative to 3s(1) for cases in which the number of unpaired 3d electrons is smaller (MnO_2) or the transition metal ion exists in a diamagnetic ground state ($K_4Fe(CN)_6$ and $Na_4Fe(CN)_6$). Also consistent with this interpretation is an analogous spectrum from Cu metal (d electron configuration $3d^{10}$) which shows a narrow, single 3s peak as observed in the ferrocyanides (see Fig. 3 and Table I).

We note at this point several other possible sources of the extra peak 3s(2), all of which can be ruled out: (1) Auger electron peaks can be distinguished by a constant kinetic energy regardless of exciting x-ray energy. Mg and Al x-rays were used for this purpose. (2) A surface contaminant or incompletely hidden portion of the sample holder could give rise to unexpected photoelectron peaks, but these should be present on all samples at the same kinetic energy and probably with varying intensity relative to Mn or Fe peaks. The 3s(2) peak does not behave in this

way. (3) If surface chemical reaction produces two different types of metal atoms, shifts of the 3s binding energies due to changes in valence electron screening could give rise to two photoelectron peaks.[10] However, in this case, both 3s and 3p peaks should show the same structure[10] and this is not observed. (We note a small effect of this kind on the 3p(1) peak of FeF_3.) (4) Quantized energy losses suffered by photoelectrons in leaving the solid can give rise to peaks on the low kinetic energy side of an elastic photoelectron peak,[13] but the loss mechanisms for 3s and 3p photoelectrons should be essentially identical due to their proximity in kinetic energy. No peak with relative intensity and separation corresponding to the 3s(2) peak is seen near the 3p(1) peaks of MnF_2 and MnO. Also, most quantized losses would contribute some inherent line width to the secondary peaks, but Table I indicates that the 3s(2) peaks are essentially equal in width to the 3s(1) peaks for MnF_2 and MnO. (5) A photoemission process resulting in simultaneous excitation of both a photoelectron and some quantized mode of excitation could give rise to such a peak.[14,15] However, the high intensity of the 3s(2) peak, the specificity of its appearance near 3s and not 3p, and the nearly equal widths of the 3s(2) and 3s(1) peaks for MnO and MnF_2 make this explanation seem unlikely.

The origins of such splittings have been considered from a theoretical point of view, with the free Mn^{2+} ion as an illustrative example.[8] The initial state is $3d^5\ {}^6S$ and the ejection of a 3s or 3p electron gives rise to final states which are denoted as $Mn^{3+}[3s]$ and $Mn^{3+}[3p]$, respectively. In first approximation, Koopmans' Theorem[1] can be used to compute binding energies. This theorem states that the binding energy of an

electron is given by its Hartree-Fock energy eigenvalue, E, calculated for the ground state configuration of Mn^{2+}. A detailed allowance for exchange predicts that for any subshell j, $E_j^{\alpha} \neq E_j^{\beta}$ (where α,β denote spin directions). Thus, two peaks are predicted as a result of photoemission from both the 3s and 3p levels. The simplest estimate of this effect treats the exchange interaction as a perturbation which splits the restricted Hartree-Fock(RHF) 3s and 3p one-electron eigenvalues, and yields the values given in Table II, line 1.[8] Spin-unrestricted Hartree-Fock (SUHF) calculations represent a higher-order estimate in that α and β electrons are permitted to have slightly different radial wave functions, but the energy splittings are not appreciably altered (see Table II, line 2). The signs of the splittings reported in Table II are such that electron kinetic energy increases to the right; that is, it requires less energy to form an anti-parallel 3sβ or 3pβ hole, and such photoelectrons are predicted to have <u>more</u> kinetic energy as a result.

This use of Koopmans' Theorem to equate binding energies to ground state energy eigenvalues is known to have shortcomings, in particular for systems with unfilled valence shells.[1] The correct definition of electron binding energy is the difference between computed total energies for initial states and final hole states [cf. Eq. (1)]. The possible final hole states are ^7S and ^5S for Mn^{3+}[3s] and ^7P and ^5P for Mn^{3+}[3p]. But unlike the other final states just given, the ^5P state can be formed in three different ways from parent d^5 terms of ^6S, ^4P, and ^4D.[1] There are thus a total of 4 final multiplet states for Mn^{3+}[3p] instead of 2 final states as found in an approximation based on Koopmans' Theorem. Such multiplet

effects rule out the simple connection of 3p splittings (or splittings of <u>any</u> non-s electron) to ground state one-electron energies.[8] The total energies of these final hole states have been calculated with two "multiplet hole theory" (MHT) methods:[8] diagonalization of the appropriate energy matrix based on Coulomb and exchange integrals for an RHF single determinant of the initial state (a frozen-orbital approximation), and more accurate multi-configuration Hartree-Fock (MCHF) calculations on the final hole states (an optimized-orbital calculation). In the frozen-orbital calculation, matrix elements were computed as linear combinations of Slater F^k and G^k integrals for the initial state; the coefficients multiplying each F^k or G^k integral were obtained from standard tables.[1] Diagonalization of this matrix gave the three ^5P eigenvectors and eigenvalues.[8,9] Separate MCHF calculations were made to obtain each optimized-orbital eigenvector and its energy eigenvalue.[8] The results of these two sets of calculations are presented in Table II, lines 4 and 5. The ^5P eigenvectors are given in Table III. The agreement between frozen-orbital and optimized-orbital splitting estimates is very good, with slightly larger values for the optimized orbitals. A comparison of lines 1 and 2 with lines 4 and 5 also confirms the essential equivalence of the MHT and Koopmans' Theorem calculations of the splittings of s electron binding energies; no such equivalence exists for non-s electron binding energies.[8]

The results of Table II are borne out qualitatively by our 3s spectra from MnF_2, MnO, and FeF_3. If we identify peak 3s(1) with a ^7S final state, and 3s(2) with ^5S, the intensity ratios of these peaks are in rough agreement with a calculated ^7S:^5S relative intensity of

7:5 = 1.4:1.0. This calculation is based on a one-electron-transition model of photoemission.[9] However, the observed separation of approximately 6 eV is only about half the value predicted by the free-ion calculations. One possible reason for the reduced experimental splittings[6] is that electron-electron correlation between electrons with like spin is partially allowed for by the exchange interaction, but no allowance is made in such theoretical calculations for correlation between electrons with unlike spins.[4] Thus, spatial[4] or energy[6] asymmetries calculated without taking correlation into account may represent slight overestimates. However, it seems doubtful that a proper allowance for correlation would account for a factor of two reduction in theoretical estimates.[8,16] Another possible effect is that of covalency in chemical bonding,[8] which will act not only to pair valence electrons, but also to delocalize them, thereby weakening their interaction with the core. This effect can be estimated from the spin-<u>and</u> orbital-unrestricted Hartree-Fock (UHF) calculations of Ellis and Freeman for the $(MnF_6)^{4-}$ cluster.[17] Their predicted splittings of energy eigenvalues, listed in Table II, line 3, show a substantial decrease from the free-ion values and rather remarkable agreement with the measured splittings in MnF_2. The reduced splitting in MnO relative to MnF_2 is consistent with known effects of covalency in that oxygen bonding is more covalent than fluorine bonding.[8] On the other hand, the larger splitting observed for FeF_3 over MnF_2 is consistent with free-ion calculations,[8] which give a greater exchange splitting for Fe^{3+} than for Mn^{2+}. The measured ratio of separations for MnF_2 and MnO_2 (1.41:1.00) is larger than the computed free-ion ratio for Mn^{2+} and Mn^{4+} (1.22:1.00), as expected from increased covalent bonding effects for oxygen ligands.[8]

The observed 3s(1):3s(2) intensity ratio of approximately 2.0:1.0 for MnF_2 and MnO is not in good agreement with the $^7S:^5S$ ratio of 1.4:1.0 obtained from a free-atom calculation based on one-electron transitions.[8,9] The 1.5:1.0 ratio for FeF_3 does agree, but the apparent surface reaction indicates that this agreement may be fortuitous. There are several reasons for a discrepancy between such simple one-electron estimates and experiment:[8] (1) If the initial and final states are described in terms of SUHF wave functions, the dipole matrix elements between 3sα and 3sβ and their corresponding p-wave continuum states may be significantly different. (2) Overlap integrals between initial and final state orbitals of passive electrons may be different for different final states. Implicit in the one-electron estimate is an assumption that these overlap integrals are unity for all final states. (3) Multi-electron transitions may be significant enough to alter observed intensity ratios from one-electron predictions.[15] (4) Bonding effects will distort initial and final states from a free-atom description, as has been found in UHF cluster calculations.[17] (5) A small fraction of the photoelectron-producing atoms may exist as surface states of different electron configuration.

In Fig. 3, we present 3s spectra for the metals Fe, Co, Ni, and Cu. The temperatures of these measurements are noted, as well as the T/T_c ratios for the ferromagnets Fe, Co, and Ni.[18] We have noted that Fe shows a splitting for temperatures below and above the Curie point, whereas paramagnetic Cu shows a single, symmetric 3s peak, as expected. Figure 3 also indicates that Ni has a 3s splitting very much like that for Fe,

and the results for Co, though not conclusive, certainly exhibit considerable broadening and asymmetry in the 3s peak. The 3p peaks for Fe (see Fig. 2), Co, Ni, and Cu can all be well approximated by a single Lorentzian with a constant tail, whereas the 3s peaks cannot. The analysis of the 3s peaks into two components as shown in Fig. 3 is somewhat arbitrary, but is analogous to the simpler results obtained for inorganic compounds. This analysis serves as a rough indicator of the magnitude of the splitting and the shape of the peak. Thus, all three ferromagnets exhibit subtle effects similar to those observed in inorganic compounds. We attribute these to a coupling of the final state 3s hole with localized 3d electrons which have some net unpaired spin or local moment. The observation of identical effects for Fe at temperatures above and below T_c[18] indicates that single-atom coupling of the 3d electrons as detected in the short time duration ($\sim 10^{-16}$ sec) of the photoemission process does not depend on the degree of long-range ferromagnetic ordering. Although this statement may seem inconsistent with the observed disappearance of the hyperfine magnetic field above T_c,[19] the latter measurements are made on a time scale of $\geqslant 10^{-12}$ sec, and thus are sensitive to the effects of a time-averaged 3d electron coupling.

Let us consider now the 3p regions of the spectra shown in Figs. 1 and 2.[8] There are several extra peaks and these have been labelled. None of these peaks are due to Auger transitions. The peaks 3p(2) and 3p(3) of $K_4Fe(CN)_6$ appear to be associated with two-electron transitions of potassium, and are not observed in similar spectra from $Na_4Fe(CN)_6$ and $(NH_4)_4$ $Fe(CN)_6$. These peaks are observed to some degree in other

potassium-containing salts such as K_2SO_4. The peaks denoted 3p(2) and 3p(3) for MnF_2, MnO_2, and FeF_3 may be connected with multiplet splittings, however. There is at least qualitative agreement with predictions from multiplet-hole-theory calculations,[8] in that peaks resulting from p electron ejection are spread out in intensity over a broad region (see Table II). We note that in a one-electron transition the intensity of each ^5P state will be proportional to the square of the coefficient of the $d^5(^6S)p^5\ ^5P$ term in the eigenvector.[8,9] Thus, the relative intensities obtained from frozen-orbital MHT calculations on Mn^{3+} are: $^5P_1$, 0.66; $^5P_2$, 0.01; and $^5P_3$, 0.32.[8,9] The $^5P_2$ peak would thus probably be too weak to observe. Spectra for MnF_2 in fact show two weaker components (3p(2) and 3p(3)) in addition to 3p(1). One of these is close to the main peak ($\sim$ 2 eV) and the other much further away ($\sim$ 17 eV). The identification of peak 3p(2) with the final state $^5P_3$ and of 3p(3) with $^5P_1$ is thus roughly consistent with non-relativistic free-ion theoretical calculations. We note, however, that any realistic theoretical treatment of 3p splittings must include spin-orbit and crystal-field effects, as well as possible decreases in the magnitudes of predicted splittings due to covalent bonding. Spin-orbit splitting of the ground state Mn3p levels will be approximately 1.3 eV in magnitude, for example.[20] Furthermore, the experimental data in the 3p regions are not good enough to assign accurate positions and intensities to the observed peaks. Thus, while it appears that peaks due to multiplet splittings may be present in the 3p regions of our spectra, further experimental and theoretical study will be necessary to assign the observed peaks to specific final hole states.

The splittings reported up to this point have been in subshells with the same principal quantum number (and thus the same approximate radial location) as the 3d electrons. Analogous effects should be observed in all core levels, although the appropriate Coulomb and exchange integrals describing the final state coupling will be decreased due to the greater average distance of separation of these inner-core and valence electrons. An approximate indicator of this decrease is given by the $2p\alpha - 2p\beta$ one-electron energy difference for atomic Fe, compared to the $3s\alpha - 3s\beta$ difference. In the SUHF calculation for line 2, Table II,[8] these values are 3.5 eV and 11.1 eV, respectively, so that one might expect an experimental splitting of ~ 6 eV for 3s peaks to be consistent with only a 2 eV splitting of 2p peaks. Also, the spin-orbit splitting of $2p_{1/2}$ and $2p_{3/2}$ levels for Mn is ~ 12 eV, so that two distinct 2p peaks will be observed. In the simplest vector-coupling model, each of these peaks will be a mixture of α and β electrons, so that, at most, the experimental expectation would be for a broadening of ~ 2 eV in the $2p_{1/2}$ and $2p_{3/2}$ photoelectron peaks. In Fig. 4, we show 2p photoelectron spectra for Fe metal and MnF_2. In analogy with the 3s splittings, we expect smaller multiplet effects for Fe than for Mn in MnF_2. As indicated, the widths of the MnF_2 peaks are 3.3 eV, or ~ 1.3 eV larger than those of Fe. This broadening is not due to surface chemical reaction, as the 3p(1) peak of MnF_2 is essentially the same width as the 3p(1) peak of Fe (2.1 eV and 2.3 eV, respectively). As mentioned previously, simple broadening or splitting of peaks due to chemical reaction will affect all core levels in a very similar way. The 2p peaks for iron are also sharper

in the sense that they are best described by a Lorentzian peak shape, whereas a broader Gaussian peak shape well approximates the MnF_2 data. Both these observations are consistent with multiplet effects of the expected magnitude on the binding energies of Mn2p electrons in MnF_2. These XPS results are also in agreement with splittings observed in x-ray emission spectra of MnF_2 and other inorganic solids.[21] $MnK\alpha_1$ and $K\alpha_2$ x-rays result from the transition $2p_{3/2} \rightarrow 1s$ and $2p_{1/2} \rightarrow 1s$, respectively. Thus, the final state is Mn with a 2p hole, just as in photoemission, and the coupling of this hole with unpaired 3d electrons will cause splitting of the resultant x-ray line. Free-ion calculations of these splittings have been made and they predict a broadening of these MnF_2 x-ray lines of ~ 2 eV,[21] in good agreement with both x-ray emission and XPS results. The experimental widths of the $K\alpha_1$ and $K\alpha_2$ x-ray lines for MnF_2 are very nearly equal,[21] in agreement with the equal widths observed in Fig. 4. The relative $K\alpha_1 : K\alpha_2$ widths are predicted by theory to be $\sim 4:3$, however.[21]

We also note that splittings of $p_{3/2}$ electron binding energies have been observed in the XPS spectra of solids containing Au, Th, U, and Pu.[22] These splittings are thought to be due primarily to crystal-field effects on metal core electronic states,[22] but no detailed theoretical analysis of this data has as yet been completed. In the broadest sense of the term "multiplet splitting," the work reported here and this earlier work[22] are representative of similar effects. That is, in both cases, the ejection of an electron from a single $n\ell$ or $n\ell j$ subshell gives rise to more than one possible final state, and the different final states have

different total energies E^h (cf. Eq. 1). The different E^h values arise from a detailed consideration of the Coulomb and exchange interactions in these final states, perhaps including contributions from atoms neighboring the metal atom. However, it is clear that the multiplet splittings reported here are primarily dependent on the various possible coupling schemes in a single-atom-like hole state, whereas crystal-field-induced splittings may be more intimately connected with the symmetry and spatial distribution of the bonds around the metal atom, regardless of the presence of unpaired electrons. For many systems with unpaired electrons, these two effects will be inseparable in an accurate theoretical analysis.

2. Gaseous 4f Metals

Similar multiplet effects should also be observed in gaseous monatomic metals with unpaired valence electrons. The interpretation of such data should be more straightforward, in the sense that crystal-field and covalent-bonding effects need not be considered. In particular, Eu, with a half-filled 4f shell, should exhibit multiplet splittings analogous to those of Mn^{2+}, with a half-filled 3d shell. Treating exchange as a perturbation, the 4sα and 4sβ one-electron energies are predicted to be different by 11.7 eV,[23] for example. Unfortunately, the 4s and 4p photoelectron intensities were too weak to permit study of these levels with the present apparatus. The 4d photoelectron intensity is much higher, however, and a photoelectron spectrum in this region is shown in Fig. 5. In order to detect small multiplet effects, we compare the Eu4d spectrum with the 4d spectra of the nearby atoms Xe and Yb. The latter two

atoms have filled outer shells and should exhibit no multiplet effects. The ground state electron configurations of these three cases are: Xe^0 - $5s^2 5p^6\ ^1S$, Eu^0 - (Xe) $4f^7 6s^2\ ^8S_{7/2}$,[24] and Yb^0 - (Xe)$4f^{14} 6s^2\ ^1S$.

The basic structure of the $4d_{3/2}$ - $4d_{5/2}$ spin-orbit doublet is observed for all three spectra in Fig. 5, and the separation of two components is close to that predicted by theory,[20] as indicated in Table IV. The increase in the linewidth of each component from Xe to Eu to Yb can be ascribed to a decrease in the lifetime τ of the 4d hole state such that $\tau_{Xe} > \tau_{Eu} > \tau_{Yb}$. Because a 4d hole can be filled by 4f electrons, it is to be expected that τ will decrease as the 4f shell is filled.

There are however, two peculiarities in the Eu spectrum of Fig. 5: the left component of the doublet has a lower relative intensity in Eu than in Xe or Yb, and the shapes of the peaks for Eu are more nearly Gaussian, as compared to Lorentzian shapes for Xe and Yb. LuF_3, a stable solid compound containing Lu^{3+} ions with a $4f^{14}\ ^1S$ electron configuration, was also studied and these results show a Lorentzian line shape for the two 4d compondnts (see Fig. 6). The relative intensities of the two components as derived by least-squares fits of the appropriate shapes are also given in Table IV. The theoretical intensity ratio for a simple spin-orbit doublet is 6:4 = 1.50:1.00. More accurate relativistic calculations yield a ratio very close to this.[25] This value is in agreement with the ratios observed for Xe, Yb, and LuF_3. The data for Eu definitely deviate from this simple model, however. No theoretical free-ion calculations are available for the Eu^{1+}[4d] hole state, but in analogy with Mn^{3+}[3p], we expect several possible final states. In the oversimplification of LS coupling, the allowed final states are $4d^9 4f^7 6s^2\ ^9D$ and

$4d^9\ 4f^7 6s^2\ {}^7D$. The ${}^9D$ state can only be formed from a parent term of $4f^7\ {}^8S$. The ${}^7D$ state can be formed from ${}^8S$, ${}^6P$, ${}^6D$, ${}^6F$, and ${}^6G$ parent terms, however. Thus, six photoelectron peaks are predicted in this model. The introduction of spin-orbit effects would no doubt increase this number.

A further peculiarity in XPS results from Eu 4d electrons is that the two-component separation is larger in Eu_2O_3 by $\sim$ 1.0 eV. Experiments on Eu_2O_3 powder yield a separation of 5.7 eV, in good agreement with previous measurements[10,26] (see Fig. 6). Intensity ratios cannot be accurately derived from the Eu_2O_3 results, due to a high intensity of inelastic scattering and probable surface reduction of a small fraction of the Eu atoms. However, the difference in separation might well be connected to bonding effects in Eu_2O_3 analogous to those discussed for Mn compounds. Thus, although it appears that the various peculiarities in Eu4d photoelectron spectra are connected to multiplet effects, no definite statements can be made without a more detailed theoretical analysis.

The 4f photoelectron spectrum of gaseous Eu is shown in Fig. 7. An intense peak is observed, with a FWHM of $\sim$ 2.0 eV. The 6s photoelectric cross section should be very small relative to 4f,[25] so it is doubtful that appreciable intensity in Fig. 7 is due to photoemission of 6s electrons. The lifetime of a 4f hole should also be very long, so that any width of the peak in Fig. 7 above the instrumental limit of $\sim$ 1.0 eV must be due to some sort of binding energy splitting. LS coupling represents a reasonable description of photoemission from 4f levels, and the final hole state must be a $4f\ {}^6 6s^2$ state which acts as a parent term for

the initial state $4f^7 6s^2\ {}^8S_{7/2}$. Only the ${}^8S_{7/2}$ initial state need be considered, as the nearest excited state is $\sim$ 1.5 eV higher in energy[24] and will not be populated at the temperatures of these experiments ($\sim$ 600°C). The only final state possible in a one-electron transition is thus $4f^6 6s^2\ {}^7F$. Spin-orbit effects will split this final state into various J components. These ${}^7F_0$, ${}^7F_1$, ${}^7F_2$,$\cdots$, ${}^7F_6$ components are spread in energy over $\sim$ 0.6 eV,[2] and this is sufficient to explain a good fraction of the extra width observed for the 4f photoelectron peak. Doppler broadening will also add a small contribution of $\sim$ 0.1 eV width. It is also possible that two-electron transitions[15] would yield $4f^6 6s^2$ final states other than ${}^7F$ or other final state configurations, such as $4f^6 6s5d$. Taken together, these effects are qualitatively consistent with the observed width of the 4f peak.

D. Conclusions

Multiplet splitting of core electron binding energies has been observed in several solids containing metal atoms with unpaired 3d electrons. The largest splittings are $\sim$ 6 eV for the 3s electrons of Mn and Fe.[8] Free-ion theoretical calculations overestimate these 3s splittings by roughly a factor of two. Calculations taking into account the effects of covalent chemical bonding[17] give excellent agreement with experiment.[8] The 3p electron binding energies also appear to show such splittings, although the theoretical interpretation of such data is more complicated.[8] The 3s photoelectron peaks for the ferromagnetic metals Fe, Co, and Ni also show evidence of such multiplet effects. For Fe, these effects are identical in both the paramagnetic and ferromagnetic states. The 2p photoelectron peaks in MnF_2 show broadening of at least 1.3 eV. These results are consistent with multiplet effects predicted from free-ion calculations, and also agree with splittings observed in x-ray emission spectra.[21]

Similar multiplet splittings are indicated in the electron binding energies of gaseous Eu. The 4d photoelectron peaks for gaseous Eu show anomalous intensity ratios and shapes when compared to similar spectra from gaseous Xe and Eu. These anomalies appear to be linked to multiplet splittings. The width of the Eu4f photoelectron peak can be explained by a consideration of multiplet effects.

ACKNOWLEDGMENTS

We wish to thank A. J. Freeman, P. S. Bagus, and J. V. Mallow for supplying us with the results of numerous theoretical calculations, and for helpful discussions. T. Novakov is gratefully acknowledged for useful comments regarding crystal-field splittings of core electron binding energies and splittings in x-ray emission spectra.

REFERENCES

* Work partially supported by the U. S. Atomic Energy Commission.

1. J. C. Slater, Quantum Theory of Atomic Structure (McGraw-Hill Book Co., Inc., New York, 1960) Vol. II.
2. J. H. Wood and G. W. Pratt, Jr., Phys. Rev. 107, 995 (1957); R. E. Watson and A. J. Freeman, Phys. Rev. 120, 1125, 1134 (1960); D. A. Goodings, Ph.D. dissertation, Cambridge University, 1960.
3. P. S. Bagus and B. Liu, Phys. Rev. 148, 79 (1966).
4. R. E. Watson and A. J. Freeman, Hyperfine Interactions, ed. by A. J. Freeman and R. B. Frankel (Academic Press, Inc., New York, 1967) p. 53.
5. A. J. Freeman, Hyperfine Structure and Nuclear Radiations, ed. by E. Matthias and D. A. Shirley (North-Holland Pub. Co., Amsterdam, 1968) p. 427.
6. C. S. Fadley and D. A. Shirley, Phys. Rev. Letters 21, 980 (1968).
7. J. Hedman, P. F. Hedén, C. Nordling, and K. Siegbahn, Phys. Letters 29A, 178 (1969).
8. C. S. Fadley, D. A. Shirley, A. J. Freeman, P. S. Bagus and J. V. Mallow, Phys. Rev. Letters 23, 1397 (1969).
9. C. S. Fadley, Ph.D. dissertation, University of California, Berkeley, 1970 (Lawrence Radiation Laboratory Report UCRL-19535).
10. C. S. Fadley, S. B. M. Hagström, M. P. Klein, and D. A. Shirley, J. Chem. Phys. 48, 3779 (1968).
11. C. S. Fadley and D. A. Shirley, Lawrence Radiation Laboratory Report UCRL-18953 (to appear in NBS J. Res.).
12. D. R. Stull and G. C. Sinke, Thermodynamic Properties of the Elements, Adv. in Chem. Ser., no. 18 (Amer. Chem. Soc., Washington, 1956).

13. L. Marton, J. Arol Simpson, H. A. Fowler, and N. Swanson, Phys. Rev. 126, 182 (1962).

14. R. K. Nesbet and P. M. Grant, Phys. Rev. Letters 19, 222 (1967).

15. M. O. Krause, T. A. Carlson, and R. D. Dismukes, Phys. Rev. 170, 37 (1968).

16. R. K. Nesbet, private communication.

17. D. E. Ellis and A. J. Freeman, to be published.

18. C. Kittel, Introduction to Solid State Physics, 3rd ed. (Wiley Pub. Co., New York, 1966).

19. See, for example, K. Johansson, E. Karlsson, L. O. Norlin, P. N. Tandon, and H. C. Jain. Hyperfine Structure and Nuclear Radiations, ed. by E. Matthias and D. A. Shirley (North-Holland Publ. Co., Amsterdam, 1968), p. 471, and D. A. Shirley, S. S. Rosenblum, and E. Matthias, op. cit., p. 480.

20. F. Herman and S. Skillman, Atomic Structure Calculations (Prentice-Hall, Inc., Englewood Cliffs, New Jersey, 1963).

21. V. I. Nefedov, Akad. Nauk. SSSR, Bull. Phys. Ser. 28, 724 (1964).

22. T. Novakov and J. M. Hollander, Phys. Rev. Letters 21, 1133 (1969); T. Novakov and J. M. Hollander, Bull. Am. Phys. Soc. 14, 524, BM4 (1969).

23. A. J. Freeman, private communication.

24. G. Smith and B. G. Wybourne, J. Opt. Soc. Am. 55, 121 (1965).

25. G. Rakavy and A. Ron, Phys. Rev. 159, 50 (1967).

26. Ö. Nilsson, C. H. Nordberg, J. E. Bergmark, A. Fahlman, C. Nordling, and K. Siegbahn, Helv. Phys. Acta. 41, 1064 (1968).

27. E. V. Sayre and S. Freed, J. Chem. Phys. 24, 1213 (1956).

Table I. Transition-metal ion electron configurations for the solids indicated in Figs. 1, 2, and 3, together with experimental separations, intensity ratios, and widths of the 3s photoelectron peaks, and the widths of the most intense 3p peaks. Accuracies of these values are ± 0.1 eV for separations and widths and ± 0.15 for intensity ratios. Values in parentheses have greater uncertainty.

Atom	Compound	Electron Configuration	3s(1)-3s(2) Separation (eV)	3s(1):3s(2) Intensity Ratio	3s(1) FWHM[a] (eV)	3s(2) FWHM[a] (eV)	3p(1) FWHM[a] (eV)
Mn	MnF_2	$3d^5\ ^6S$	6.5	2.0:1.0	3.2	3.2	2.1
	MnO	$3d^5\ ^6S$	5.7	1.9:1.0	3.6	3.5	2.8
	MnO_2[b]	$3d^3\ ^4F$	4.6	2.3:1.0	3.9[c]	3.9[c]	2.6
Fe	FeF_3[d]	$3d^5\ ^6S$	7.0	1.5:1.0	4.5[c]	4.5[c]	3.6[d]
	Fe	$(3d^6 4s^2)$	(4.4)	(2.6:1.0)	(3.5)	(4.0)	2.3
	$K_4Fe(CN)_6$	$(3d^6)$	---	> 10:1	3.5	---	2.9
	$Na_4Fe(CN)_6$	$(3d^6)$	---	> 10:1	3.2	---	2.6
Co	Co	$(3d^7 4s^2)$	---	---	4.3	---	2.5
Ni	Ni	$(3d^8 4s^2)$	(4.2)	(7.0:1.0)	(3.2)[c]	(3.2)[c]	3.4[e]
Cu	Cu	$(3d^{10} 4s^1)$	---	> 20:1	3.6	---	4.2[e]

[a]FWHM of symmetric peak shape, excluding asymmetry introduced by the inelastic tail.

[b]Probably slightly reduced; often a non-stoichiometric compound.

[c]FWHM for 3s(1) and 3s(2) constrained to be equal.

[d]Probably slightly reduced (see Fig. 1).

[e]The primary source of increased width for these peaks is spin-orbit splitting into $3p_{1/2}$ and $3p_{3/2}$ components.

Table II. Theoretical predictions of 3s and 3p electron binding energy splittings for a $Mn^{2+}3d^5\ ^6S$ initial state. These values are taken from Ref. 8. The units are eV.

	Final state:	$Mn^{3+}[3s]$			$Mn^{3+}[3p]$		
	Koopmans' Theorem Description:	3sα hole	3sβ hole		3pα hole		3pβ hole
(1)	RHF + exchange perturbation (Mn^{2+})	11.1	0		13.5		0
(2)	SUHF (Mn^{2+})	11.3	0		13.7		0
(3)	UHF, $(MnF_6)^{4-}$ cluster (ref. 17)	6.8	0		8.1		0
	Multiplet Description:	^5S	^7S	$^5P_1$	$^5P_2$	$^5P_3$	^7P
(4)	MHT, Frozen orbital[a]	13.3	0	22.4	8.5	3.6	0
(5)	MHT, Optimized orbital[b]	14.3	0	23.8	9.4	4.0	0

[a]Orbitals obtained from an RHF calculation on $Mn^{2+}\ 3d^5\ ^6S$.

[b]Values based on multiconfiguration Hartree-Fock calculations for $Mn^{3+}[3s]$ and $Mn^{3+}[3p]$.

Table III. Frozen-orbital eigenvectors for the three ^5P states of Mn^{3+} $3p^5$ $3d^5 \equiv Mn^{3+}[3p]$. Eigenvalues relative to the ^7P state are given in Table II.

State: / Expansion coefficients:	$^5P_1$	$^5P_2$	$^5P_3$
$C(d^5(^6S)p^5\ ^5P)$	0.816	-0.110	0.567
$C(d^5(^4D)p^5\ ^5P)$	-0.439	0.519	0.733
$C(d^5(^4P)p^5\ ^5P)$	-0.375	-0.847	0.375

Table IV. Summary of results for 4d photoelectron spectra of Xe, Eu, Yb, and Lu in various samples. A comparison is also made to the theoretical spin-orbit splitting of $4d_{3/2}$ and $4d_{5/2}$ components. Accuracies of these values are ± 0.1 eV for separations and widths and ± 0.15 for intensity ratios.

Sample	4d component FWHM[a] (eV)	4d Component separation (eV)	Theo. spin-orbit splitting[b] (eV)	Component separation / Theo. spin-orbit	4d component intensity ratio
Xe(gas)	1.07[c]	1.96	2.10	.94	1.47:1.00
Eu(gas)	3.78[d]	4.77	5.40[e]	.88	2.44:1.00
Eu_2O_3(solid)	3.63[c]	5.73	5.40[e]	1.06	---
Yb(gas)	5.41[c]	8.43	9.20	.92	1.49:1.00
LuF_3(solid)	4.23[c]	10.24	10.00[e]	1.02	1.75:1.00[f]

[a]The two 4d components were assumed to have equal widths. FWHM values are for a symmetric peak shape, excluding asymmetry introduced by the inelastic tail.

[b]Taken from Ref. 20.

[c]Analysis with Lorentzian-based peak shapes.

[d]Analysis with Gaussian-based peak shapes.

[e]Value obtained by interpolation from those given in Ref. 20.

[f]The accuracy of this ratio is not as high as for the other ratios reported, due to inelastic scattering effects.

FIGURE CAPTIONS

Fig. 1. Photoelectron spectra from MnF_2, MnO, and MnO_2 in the kinetic-energy region corresponding to ejection of Mn 3s and 3p electrons by MgKα x-rays.

Fig. 2. Photoelectron spectra from FeF_3, Fe metal, $K_4Fe(CN)_6$ and $Na_4Fe(CN)_6$ in the kinetic-energy region corresponding to ejection of Fe 3s and 3p electrons by MgKα x-rays.

Fig. 3. 3s photoelectron spectra from Fe metal, Co metal, Ni metal, and Cu metal. MgKα x-rays were used for excitation. Binding energies corresponding to the intense peaks produced by $MgK\alpha_{1,2}$ x-rays are also indicated. The vertical bars on each point indicate statistical error limits.

Fig. 4. 2p photoelectron spectra from Fe metal and MnF_2. MgKα x-rays were used for excitation. The Fe data have been analyzed into two Lorentzian components and the MnF_2 data into two Gaussian components.

Fig. 5. 4d photoelectron spectra from gaseous Xe, Eu, and Yb, produced by excitation with MgKα x-rays. The theoretical spin-orbit splitting into $4d_{3/2}$ and $4d_{5/2}$ components is also indicated. Theoretical values are from Ref. 20. (See Table IV.)

Fig. 6. 4d photoelectron spectra from solid Eu_2O_3 and LuF_3, produced by excitation with MgKα x-rays. (See Table IV.)

Fig. 7. 4f photoelectron spectrum from gaseous Eu, produced by excitation with MgKα x-rays.

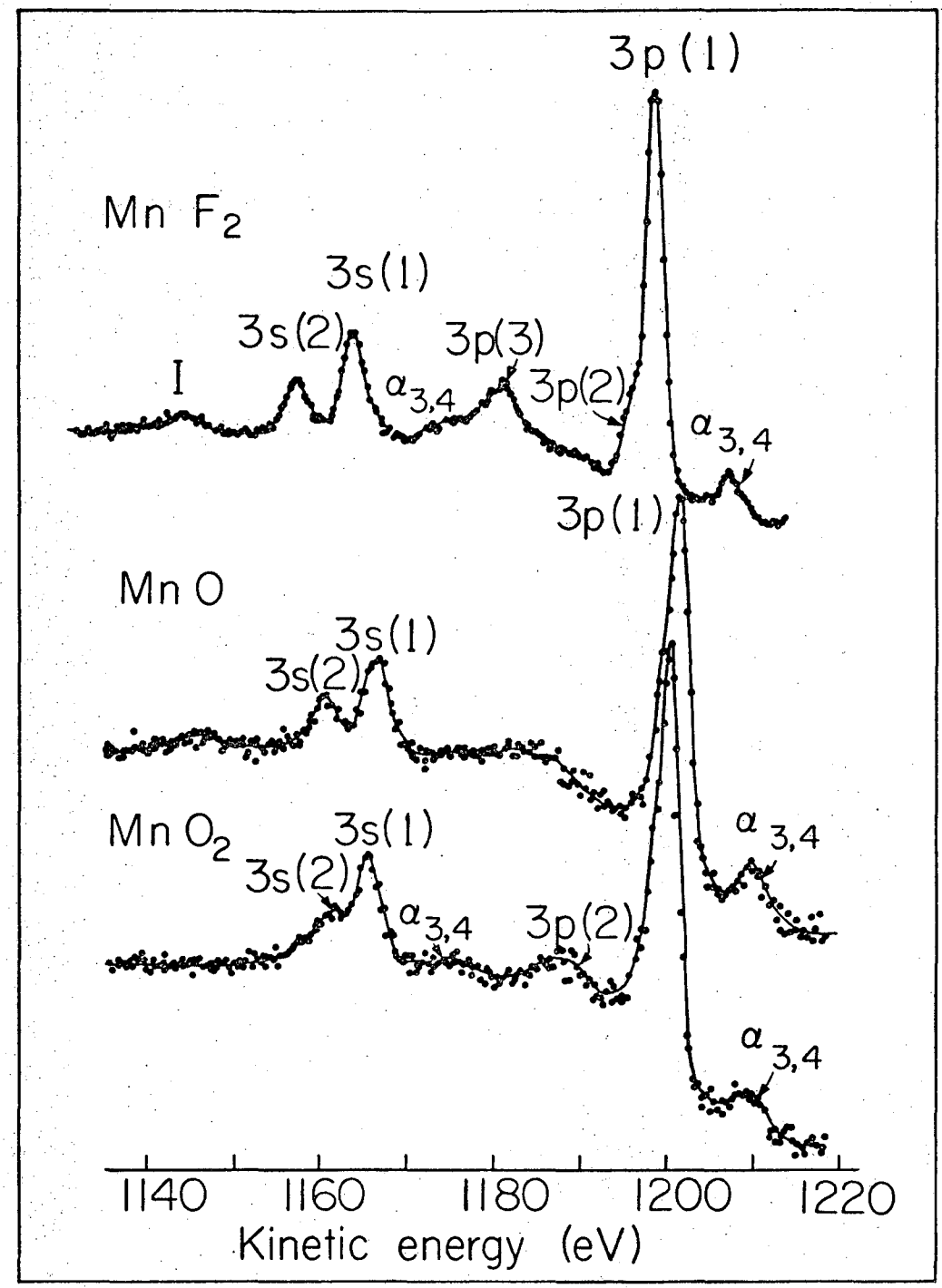

XBL703-2529

Fig. 1

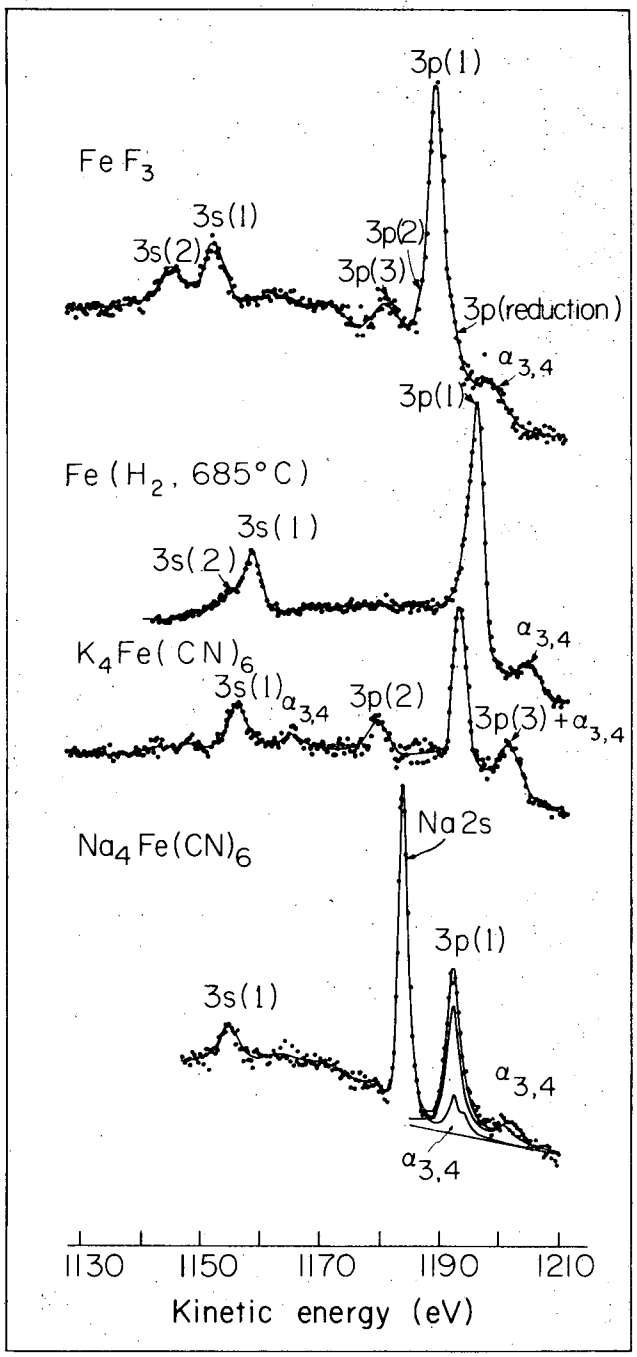

XBL 703-2530

Fig. 2

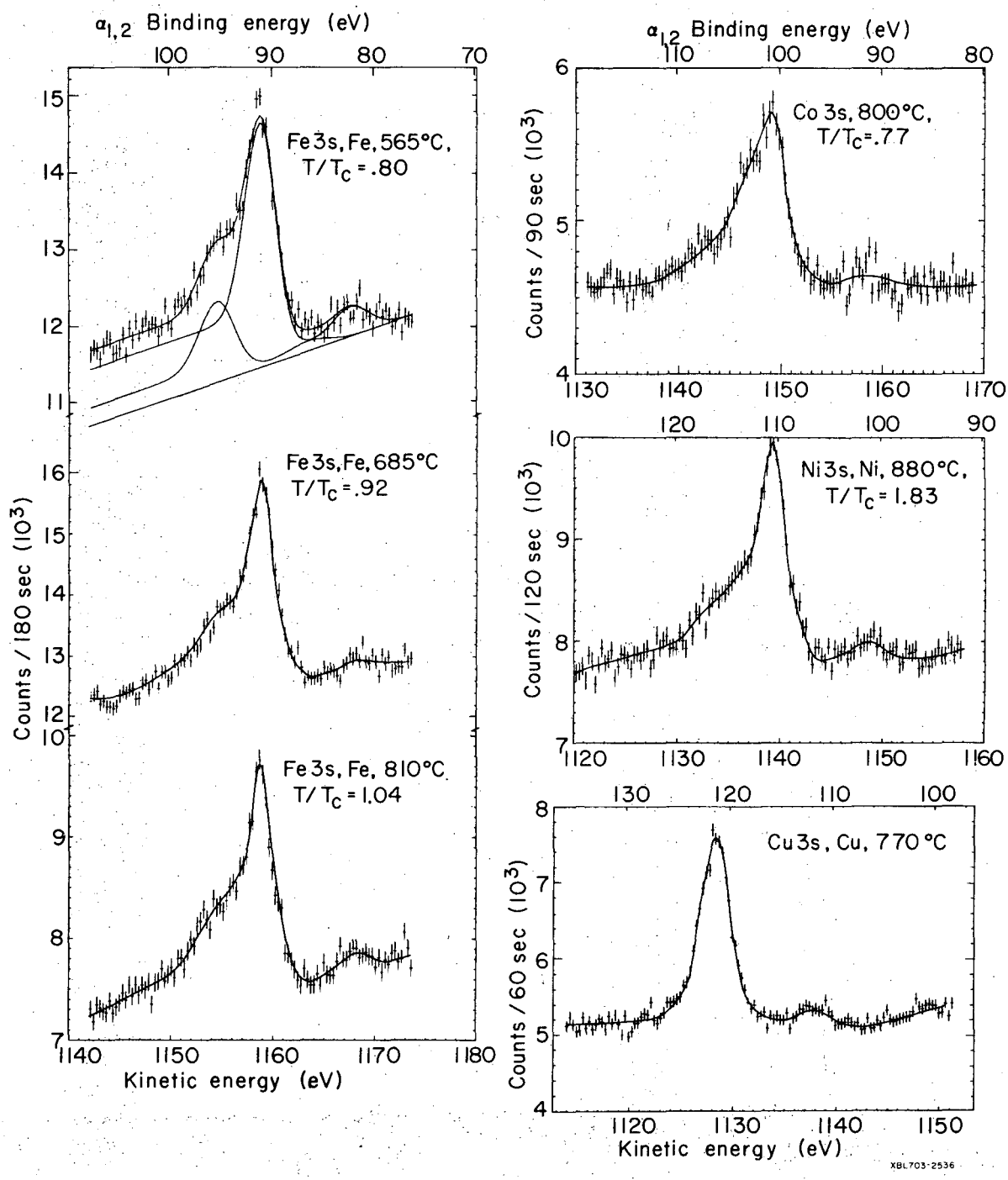
α1,2 Binding energy (eV)
Fe 3s, Fe, 565°C, T/Tc = .80
Fe 3s, Fe, 685°C T/Tc = .92
Fe 3s, Fe, 810°C T/Tc = 1.04
Counts / 180 sec (10³)
Kinetic energy (eV)
Co 3s, 800°C, T/Tc = .77
Counts / 90 sec (10³)
Ni 3s, Ni, 880°C, T/Tc = 1.83
Counts / 120 sec (10³)
Cu 3s, Cu, 770°C
Counts / 60 sec (10³)
XBL703-2536

Fig. 3

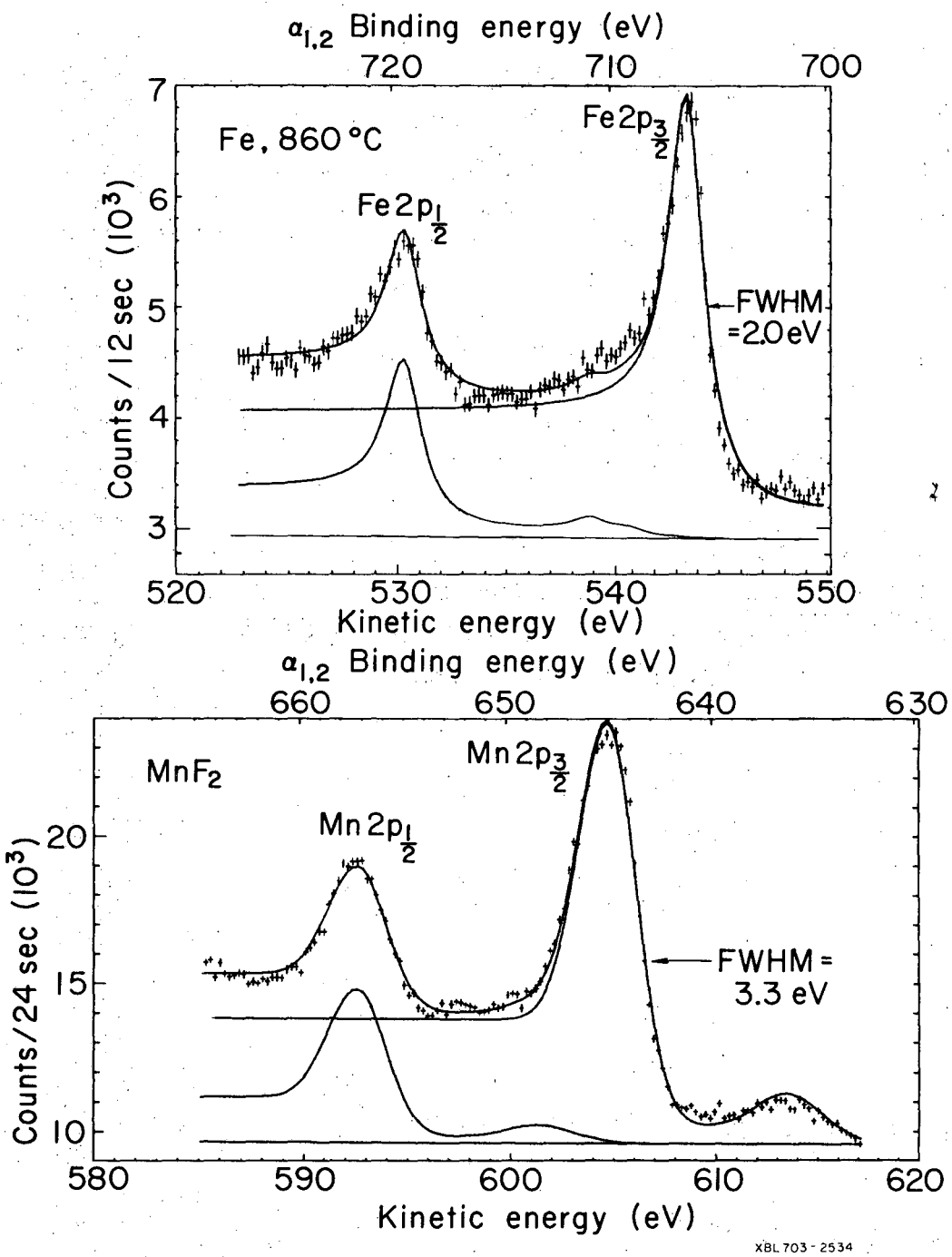
α1,2 Binding energy (eV)
720
710
700
Fe, 860 °C
Fe2p3/2
Fe2p1/2
FWHM =2.0 eV
Counts / 12 sec (10³)
7
6
5
4
3
520
530
540
550
Kinetic energy (eV)
α1,2 Binding energy (eV)
660
650
640
630
MnF2
Mn2p3/2
Mn2p1/2
FWHM = 3.3 eV
Counts/24 sec (10³)
20
15
10
580
590
600
610
620
Kinetic energy (eV)
XBL 703 - 2534

Fig. 4

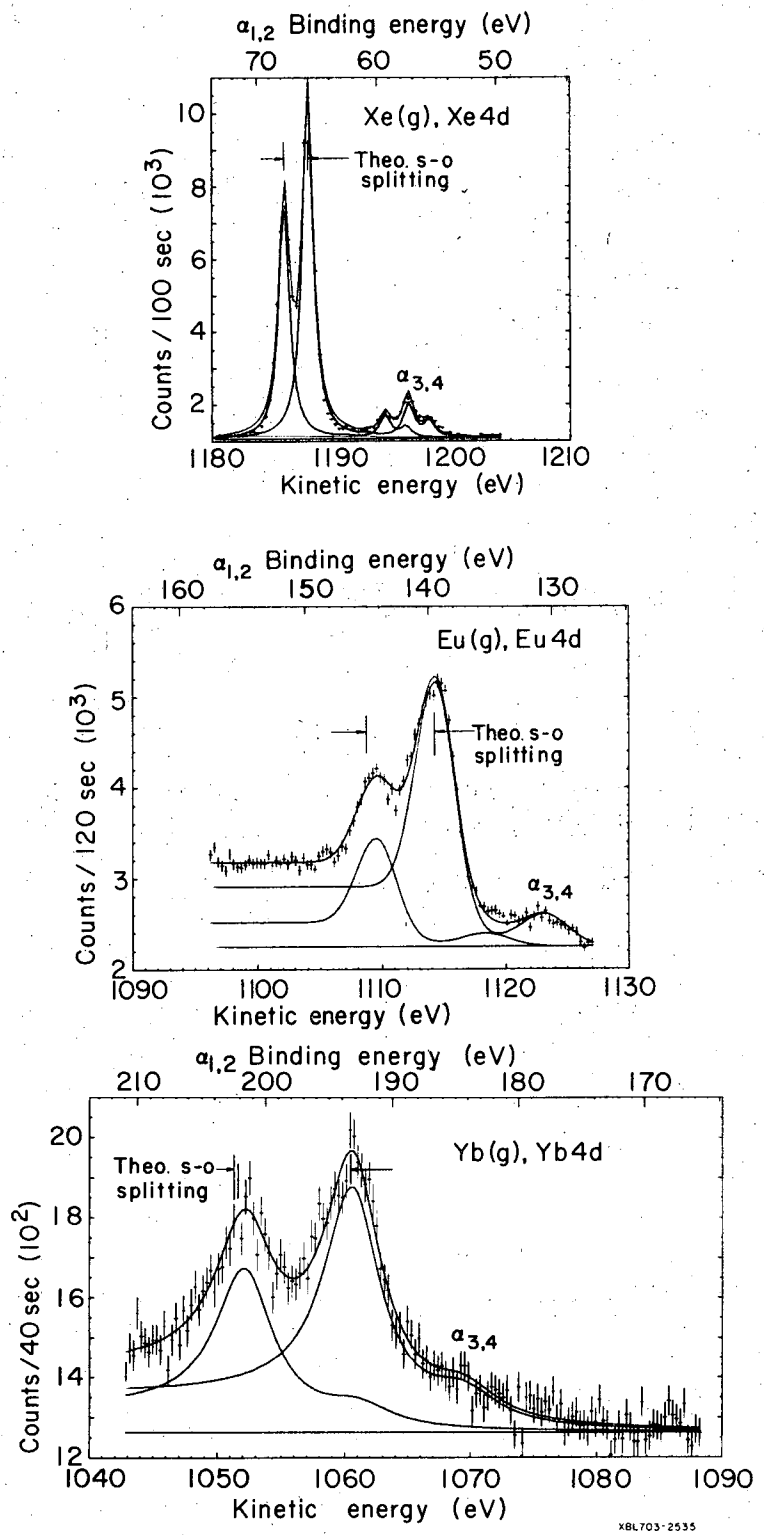
α1,2 Binding energy (eV)
70
60
50
Xe(g), Xe4d
Theo. s-o splitting
α3,4
Counts / 100 sec (10^3)
10
8
6
4
2
1180
1190
1200
1210
Kinetic energy (eV)
α1,2 Binding energy (eV)
160
150
140
130
Eu(g), Eu4d
Theo. s-o splitting
α3,4
Counts / 120 sec (10^3)
6
5
4
3
2
1090
1100
1110
1120
1130
Kinetic energy (eV)
α1,2 Binding energy (eV)
210
200
190
180
170
Yb(g), Yb4d
Theo. s-o splitting
α3,4
Counts/40 sec (10^2)
20
18
16
14
12
1040
1050
1060
1070
1080
1090
Kinetic energy (eV)
XBL703-2535

Fig. 5

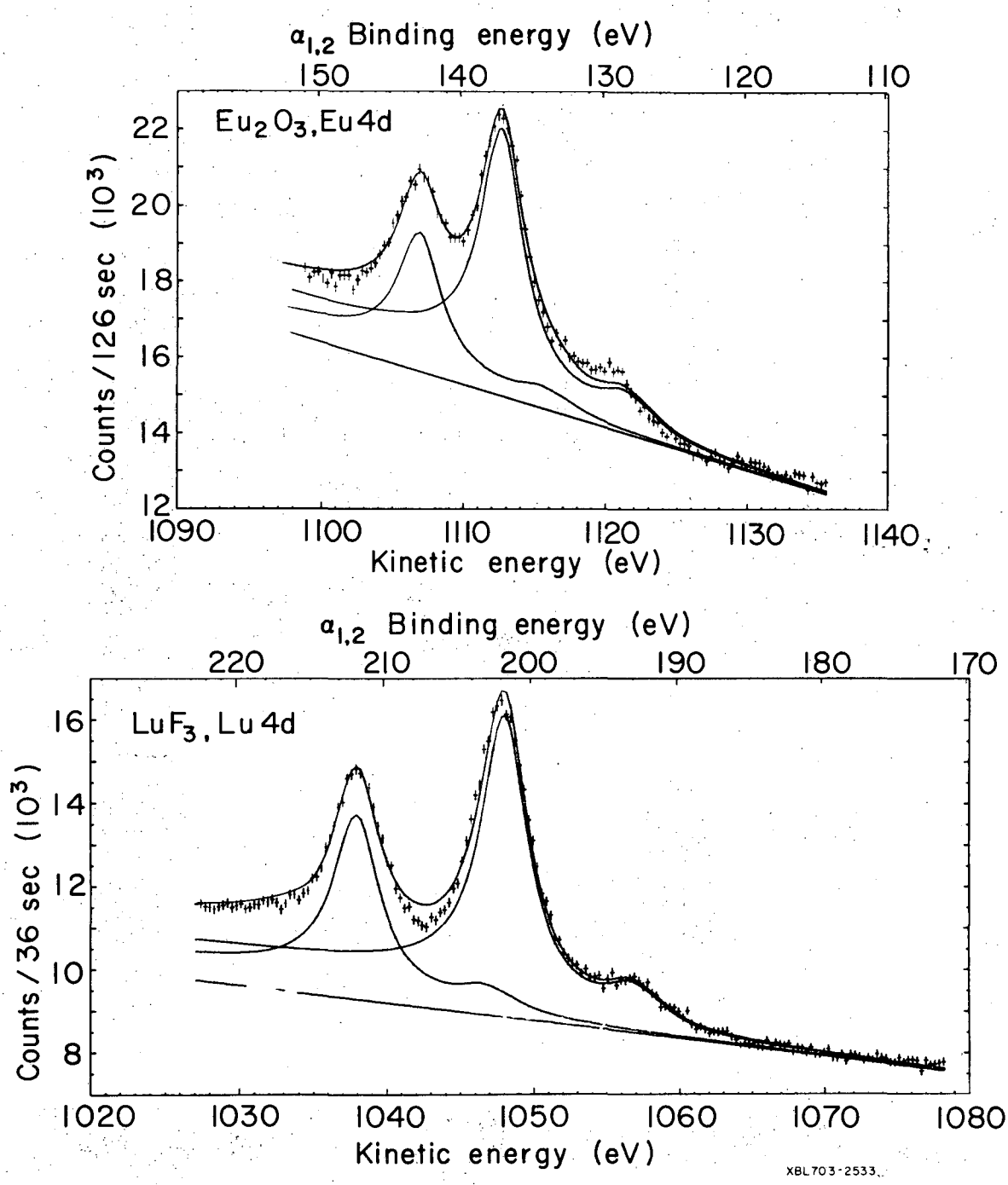
$\alpha_{1,2}$ Binding energy (eV)
150
140
130
120
110
Eu_2O_3, Eu 4d
Counts / 126 sec (10^3)
22
20
18
16
14
12
1090
1100
1110
1120
1130
1140
Kinetic energy (eV)
$\alpha_{1,2}$ Binding energy (eV)
220
210
200
190
180
170
LuF_3, Lu 4d
Counts / 36 sec (10^3)
16
14
12
10
8
1020
1030
1040
1050
1060
1070
1080
Kinetic energy (eV)
XBL703-2533

Fig. 6

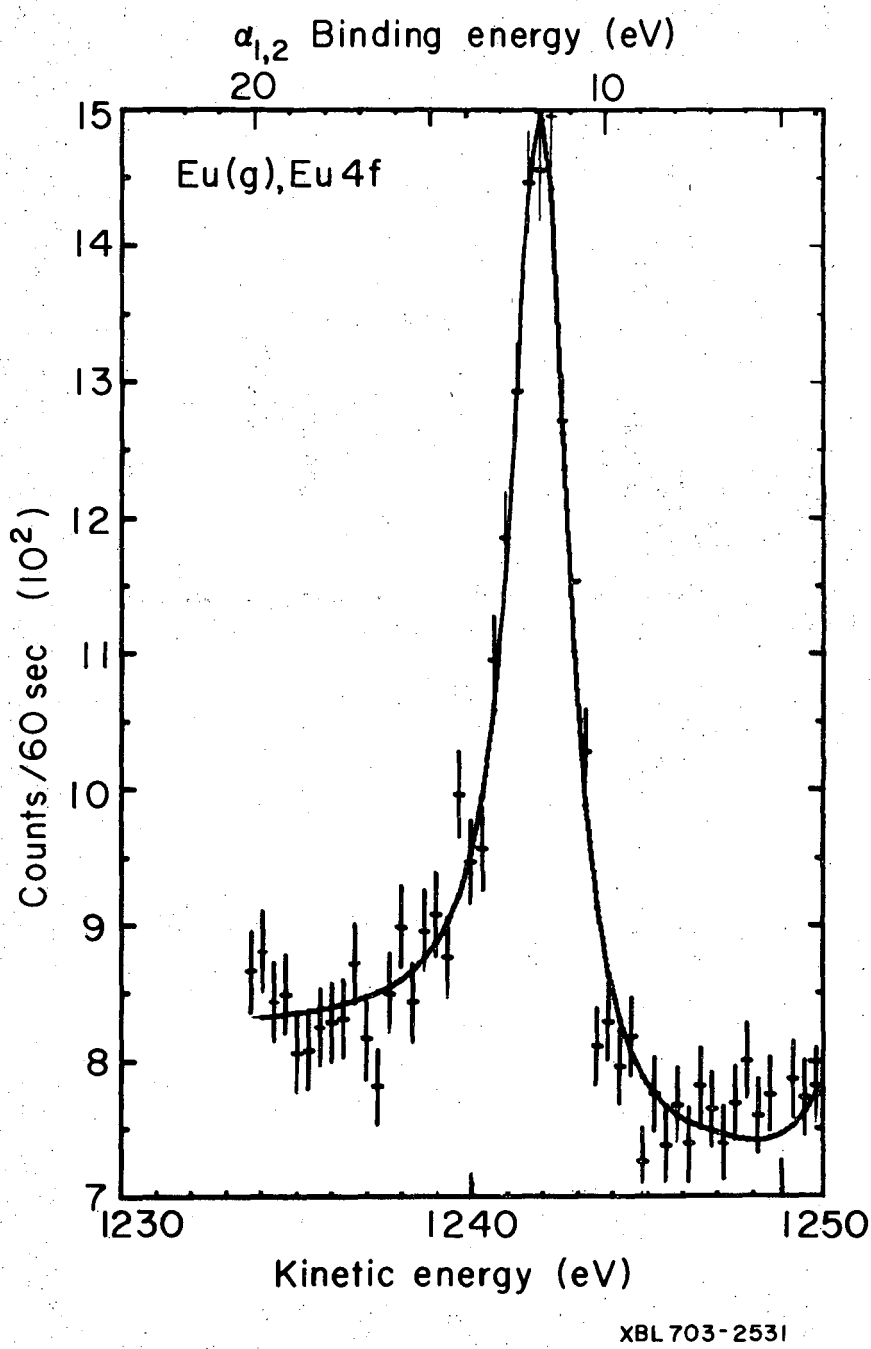
$\alpha_{1,2}$ Binding energy (eV)
20
10
Eu(g),Eu 4f
15
14
13
12
11
10
9
8
7
Counts/60 sec (10^2)
1230
1240
1250
Kinetic energy (eV)
XBL 703-2531

Fig. 7

LEGAL NOTICE

This report was prepared as an account of Government sponsored work. Neither the United States, nor the Commission, nor any person acting on behalf of the Commission:

A. Makes any warranty or representation, expressed or implied, with respect to the accuracy, completeness, or usefulness of the information contained in this report, or that the use of any information, apparatus, method, or process disclosed in this report may not infringe privately owned rights; or

B. Assumes any liabilities with respect to the use of, or for damages resulting from the use of any information, apparatus, method, or process disclosed in this report.

As used in the above, "person acting on behalf of the Commission" includes any employee or contractor of the Commission, or employee of such contractor, to the extent that such employee or contractor of the Commission, or employee of such contractor prepares, disseminates, or provides access to, any information pursuant to his employment or contract with the Commission, or his employment with such contractor.

TECHNICAL INFORMATION DIVISION
LAWRENCE RADIATION LABORATORY
UNIVERSITY OF CALIFORNIA
BERKELEY, CALIFORNIA 94720